TRANSFORMING A CORNER OF A LIGHT-FRAME WOOD STRUCTURE TO A SET OF NONLINEAR SPRINGS[1]

Kevin M. Groom[2]
Graduate Research Assistant

and

Robert J. Leichti
Associate Professor

Department of Forest Products
Oregon State University
Corvallis, OR 97331

(Received March 1993)

ABSTRACT

The computational efficiency of a full-structure model for a light-frame building is enhanced by replacing the continuum of the detailed connections with rotational and translational nonlinear springs that are energetically equivalent between two bounds. This study examines the transformation from the physical exterior-wall-to-exterior-wall connection (a corner) of a light-frame wood structure, first, to a two-dimensional finite-element model and, then, to a set of nonlinear springs. Typical light-frame details are used as the starting point, and the product is the characteristic moment-rotation and load-displacement relationships for a 24-inch segment of the corner.

Keywords: Finite element, connections, light-frame model, light-frame construction.

INTRODUCTION

Although light-frame wood buildings are the primary form of residential construction in the United States, only recently have the load-sharing capabilities of the various substructures in such buildings been studied. The preferred way of analyzing a complete wood structure is the finite-element method. However, modeling such a complex structure in sufficient detail to accurately predict reactions and deformations requires either a model with many degrees of freedom (dof) or a reduced, but energetically equivalent model. With respect to computational time and efficiency, the latter is the obvious choice.

One aspect of creating a reduced structural model is the development of energetically equivalent intercomponent connections. Intercomponent connections join the various substructures together and play a vital role in the behavior of the structure. Previous research has shown that the nonlinear characteristics of the intercomponent connection result from the nails (Jenkins et al. 1979; Polensek and Schimel 1986; Polensek and Bastendorff 1987).

The main objective of this paper is to present a technique for reducing the number of dof from a detailed finite-element model of an intercomponent connection to a set of energetically equivalent nonlinear springs that exhibit the same moment-rotation and load-displacement relationships between two bounds as the actual framing system. These springs can be used subsequently in a full-structure model to replace the detailed modeling of the intercomponent connection. This paper presents the development of the detailed finite-element model, the verification of the finite-element results

[1] This is Paper 2930 of the Forest Research Laboratory, Oregon State University, Corvallis, OR.

[2] Present address: Research Specialist, Oregon Department of Transportation, Salem, OR 97310.

by comparison with full-scale testing, and the subsequent reduction to a set of nonlinear springs. The specific connection presented is a corner where one exterior wall joins an orthogonal exterior wall.

OVERVIEW OF THE ANALYSIS

This study was part of a larger project that demonstrated the method for modeling a full structure to determine its load-sharing characteristics (Kasal 1992). For that project, the global full-structure model by Kasal (1992) was compared with the results of a full-scale test performed on a single-story light-frame wood structure (Phillips 1990).

The structure consisted of four exterior walls and two interior partitions, each orthogonal to the adjoining walls. Each of the four corners was fastened together in the same way; therefore, one model of the exterior-wall-to-exterior-wall connection was sufficient to provide the needed nonlinear springs for the full-structure model.

The physical connection consisted of three Douglas-fir studs, plywood exterior siding, and gypsum board on the interior surfaces of the walls. Figure 1 shows the connection as well as the next adjacent stud on each wall. Wall I was the end wall (Phillips 1990) and was oriented parallel to the plane of the applied loads in the structural tests. Wall II was the one to which the loads were applied in the full-structure tests.

The process of replacing the continuum with a set of nonlinear springs is described by three steps:

- Identify the required rotations and translations.
- Develop a detailed finite-element model of the connection and verify the calculation.
- If necessary, modify the finite-element model and calculate the characteristic load-displacement and moment-rotation relationships by imposing the appropriate boundary conditions.

In this project, the connection stiffnesses required for the full-structure model included

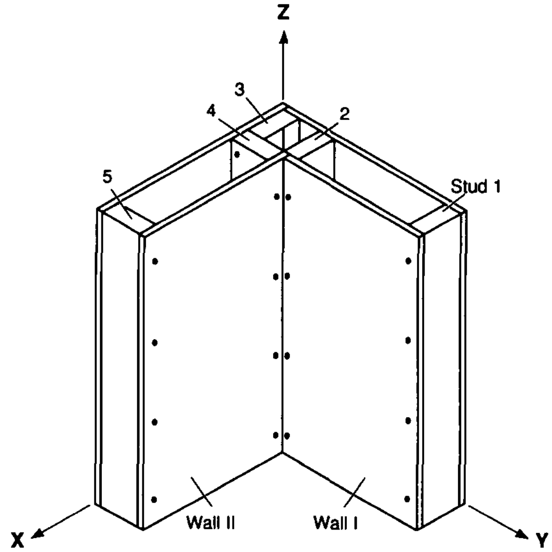

FIG. 1. Detail of exterior-wall-to-exterior-wall connection used for testing.

the rotational stiffness as the connection was both opened and closed (Kasal 1992). In addition, two separation stiffnesses were also required to make the model complete: Wall I pulled away from Wall II, and Wall II pulled away from Wall I.

The corner connection was built and tested in the opening and closing modes. The actual test specimen was then modeled according to the finite-element method, which yielded moment-rotation relationships for comparison with those derived with the experimental corners. The material properties used in the finite-element model were then modified to represent the properties of the materials in the actual structure as described by Phillips (1990). The results were the characteristic properties of moment-rotation and load-displacement for the quasi-superelements, which were nonlinear springs.

DEVELOPING AND VERIFYING THE FINITE-ELEMENT MODEL

Corner fabrication and tests

The test involved rotating the intercomponent connection so that the two walls opened

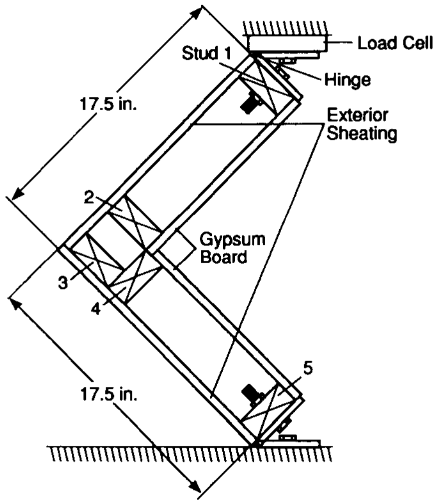

FIG. 2. Apparatus used to test the exterior-wall-to-exterior-wall connection.

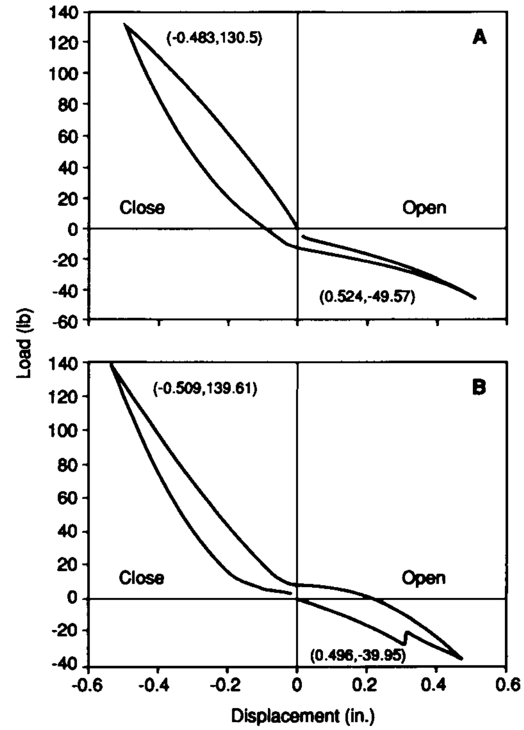

FIG. 3. Typical values of load vs. displacement for tests of the exterior-wall-to-exterior-wall connection: (A) close-open-close and (B) open-close-open.

and closed relative to one another. The testing setup used to evaluate the exterior-wall-to-exterior-wall connection is shown in Fig. 2.

The studs were cut to a length of 24 in. and ran the full height of the connection. Studs 3 and 4 were fastened together with five 16d nails spaced 6 in. o.c. The gypsum wallboard (½-in.) was fastened to the studs with four drywall nails per row, spaced 6 in. o.c. Six rows of 6d nails fastened the exterior sheathing (½-in., T1-11) to the studs. Studs 1, 2, and 5 and the xz surface of Stud 3 (see Fig. 1) each had four 6d nails spaced 6 in. o.c. The edges of Studs 3 and 4 each had five 6d nails spaced 6 in. o.c. to fasten the exterior sheathing to them. All of the nails used in the connection were hand-driven without the use of pilot holes. The outer layer of the exterior sheathing and the paper on the gypsum board both had the fibers running parallel to the length of the studs. The interior corner was not taped or finished.

The load was monitored by a load cell mounted between the hinge and the crosshead of the testing machine. The displacement measured was that of the crosshead as it was lowered or raised to load the connection.

The crosshead speed in both directions was 0.1 in./min. Although the global model of the complete structure did not require cyclic behavior, a load and fully reversed load were applied.

A total of six assembled corners were tested. The first corner was loaded in closing until the crosshead was lowered 0.5 in. The crosshead was then raised 1.0 in. to open the corner, giving a net crosshead movement of 0.5 in. Finally, the crosshead was brought back to the original unloaded position to complete the hysteresis loop. The next specimen was loaded in the opposite sequence; the corner was first loaded to open, then closed, and finally opened to the neutral position. This pattern was followed until each corner was tested.

Typical results of the testing are shown as the hysteresis loops in Fig. 3. The average hysteresis loops of the exterior-wall-to-exterior-wall connection were used to verify the finite-element model.

Developing the corner model

The finite-element model was devised to predict the behavior of the corner connection under the test conditions. Comparison of the experimental results with the model served to verify that the model was an acceptable predictor of corner behavior.

Studs and sheathing materials.—The wood and gypsum wallboard were modeled using four-node plane-stress isoparametric solid elements. Each node had two dof, which were translations in the x- and y-directions. Material properties consisted of two moduli of elasticity (E_x and E_y), Poisson's ratio (ν_{xy}), and the shear modulus (G_{xy}) (Delsalvo and Gorman 1989).

The plywood and gypsum board were tested in bending to establish the necessary material properties for the finite-element model. The method followed the guidelines outlined in ASTM D3043-87 (ASTM 1989). This method was used for both the exterior sheathing and the gypsum board because ASTM C473-87a (ASTM 1990), Standard Test Methods for Physical Testing of Gypsum Board Products and Gypsum Lath, does not provide test methods for determining the modulus of elasticity (E) of gypsum board sheathing.

The values for Poisson's ratio and the shear modulus for the sheathing materials were obtained from tests performed by Polensek and Schimel (1986). Material properties for the studs were obtained from the data of Bodig and Jayne (1982).

Nails and gaps.—Each nail in this model was represented with a pair of two-node, nonlinear, force-displacement elements (Fig. 4). These elements have only one dof per node, which is a translation in either the x- or y-direction. Each element can be thought of as a spring that either elongates under tension or becomes more compact under compression. Each nail in the model required a separate spring element to represent the shear and withdrawal resistances. The force-displacement relationships were defined by piecewise linear curves such as that in Fig. 4. The load-slip relationships were obtained for the nails from two sources: Phillips (1990) provided load-slip results in tests performed on a 16d nail joint fastening two Douglas-fir studs; the load-slip relationships for the drywall and 6d nails used to fasten the gypsum board and exterior sheathing to the studs were provided from the data of Polensek and Bastendorff (1987). The load-withdrawal curve used for the 16d nail was taken from Groom (1992).

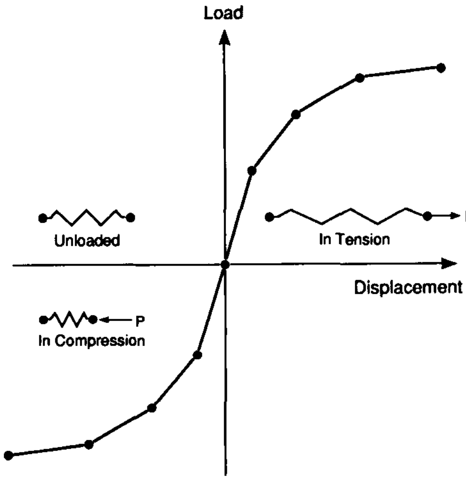

FIG. 4. Two-node, nonlinear, force-displacement element used to model the nails and gaps.

The gaps between the sheathing and the studs were modeled by force-displacement curves made up from load-withdrawal curves and the associated pull-through data of Groom (1992). The two curves were combined in series so that each part carried the same load and could displace independently of the other, thereby representing the actual behavior of the sheathing joint.

Assembling the model.—The two-dimensional finite-element mesh used to model the exterior-wall-to-exterior-wall connection is shown in Fig. 5. The boundary conditions were accurately modeled by fixing only one node (Node A, which served as the corner of Stud 1) against translation. This node was fixed in the x- and y-directions but was allowed to rotate about the z-axis (see Fig. 1), thereby simulating the hinge action of the test fixture. The finite-element loading was accomplished by forcing Node B (the corner node of Stud 5) in

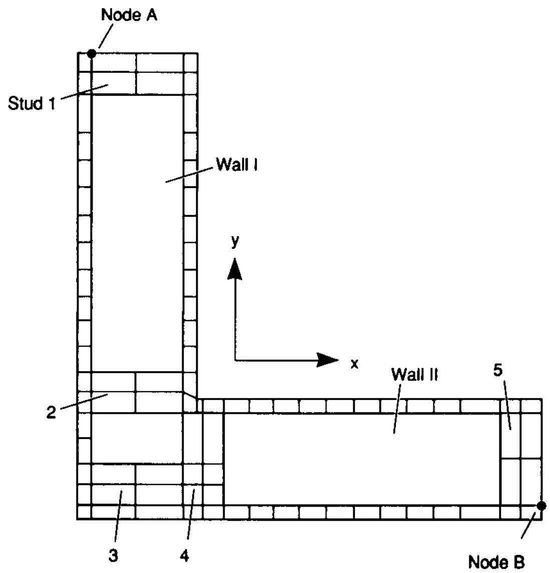

FIG. 5. Finite-element mesh used in the exterior-wall-to-exterior-wall connection model.

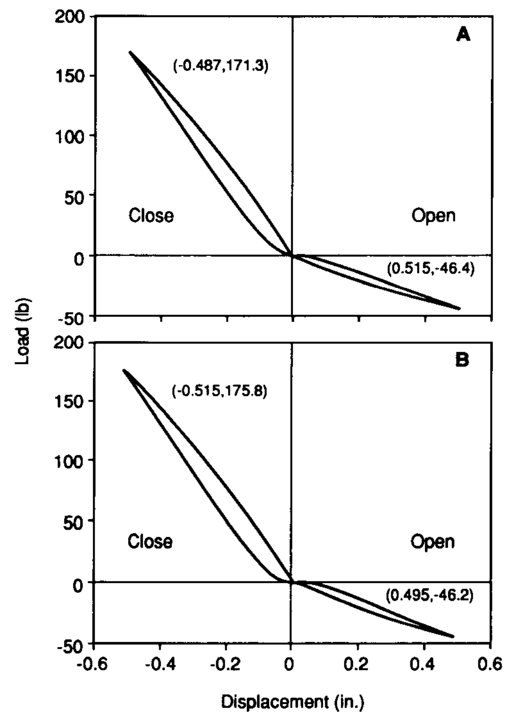

FIG. 6. Load vs. displacement loops obtained from a finite-element model of the exterior-wall-to-exterior-wall connection when the loading sequence is (A) close-open-close and (B) open-close-open.

a straight line toward Node A. The reaction loads at Node B were recorded, and the resultant load in the line of the imposed displacement represented the load recorded by the load cell.

Verification of the corner model

Close-open-close.—The first case simulated the corner subjected to hysteresis loading initiated by closing the connection. The hysteresis loop in Fig. 6A is the result of 40 load steps. Ten load steps closed the corner a total of about 0.5 in. Twenty load steps then brought the corner back through the zero displacement point and continued until the connection was open a distance of 0.5 in. Finally, the connection was brought back to the starting position to complete the hysteresis loop.

Most of the bending resulted from the sheathing materials flexing while the studs remained undeformed. Models of typical deformations of the corner in open and closed position are shown in Fig. 7.

Figure 6A shows the load-displacement relationship at Node A as the model was loaded. This curve is comparable in shape to the corresponding curve (Fig. 3A) derived from closing the actual corner specimens, although the load values for the simulation of the closing portion of the curves tended to be high. The average loadhead displacement and load in the actual specimens were 0.487 in. at 118.1 lb in closing and 0.515 in. at 47.8 lb in opening. At the same displacement values, the finite-element model predicted a closing load of 171.3 lb (45.0% error) and an opening load of 46.4 lb (2.9% error).

The large error with closing and the small error with opening are related to the assumptions of the model; all gaps between the materials were assumed to be zero. Therefore, when the model was forced into closure, the simulated wallboard and studs that made up the corner assembly were instantaneously resisting the movement. The character of the actual connection was different in that gaps existed between the materials, a result of imperfect construction. These gaps could have arisen from warped or twisted members, cuts that were not perfectly straight, and misalignment of the materials during construction. Therefore, when the actual connection was closing, not all of the materials were making contact from the start. As a result, the resisting load of the actual connection was lower than that of the finite-element model. When the model was loaded in tension, forcing the simulated connection to open, the status of the initial gaps did not play a role because the materials were continuously separating.

Open-close-open.—The second case simulated was that of the corner connection being subjected to a hysteresis loading initiated by opening the connection. The boundary conditions for this case were identical to those of the previous case. The loading was accomplished similarly except that the load path was started by opening the connection instead of closing it. Forty load steps were used to open, close, and return the connection to the unloaded position.

Figure 6B shows the load-displacement relationship for the simulated loadhead. The curve begins at the origin; as the connection opens, the curve proceeds until a displacement of 0.495 in. and a load of 46.2 lb are reached. (The average of the three tests when actual specimens were loaded in the same sequence was a load of 42.8 lb for the same displacement, indicating that the model was in error by 7.9%.) The model was then loaded in compression, closing the connection until the loadhead moved 0.515 in. past the starting position. That displacement required a load of 175.8 lb for the finite-element model and 140.5 lb for the average load of the three tests, indicating that the model was in error by 25.1%. Again, because of the effects of the gaps in the actual specimens, the model performed more like those specimens when loaded in tension than when loaded in compression.

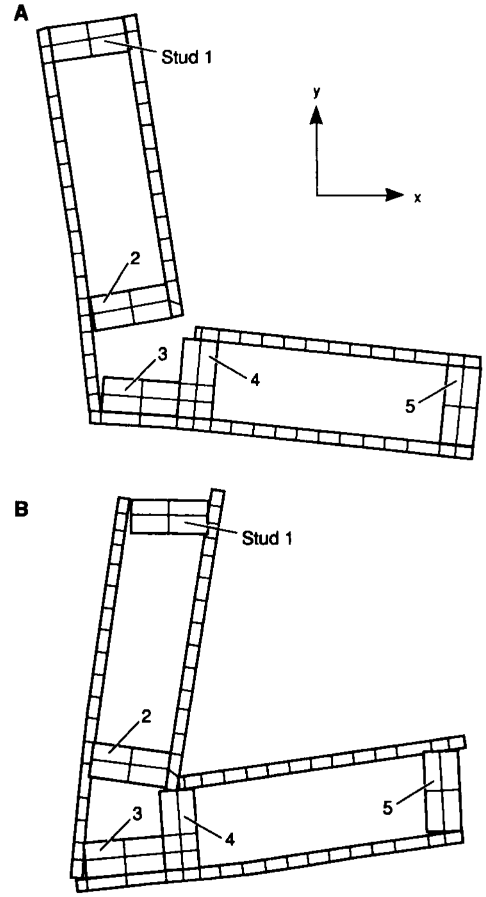

FIG. 7. Finite-element model of the deformed corner in the (A) open and (B) closed positions.

TRANSFORMING THE CONTINUUM

The nailing schedule and material properties of the finite-element model were then modified to correspond with the connection details as described by Phillips (1990) or Groom (1992). However, the finite-element mesh was not revised. It should be noted that these results were for a 24-in. section of the connection. If these results were to be expressed as springs appearing every 12-in. in the global structural model, then the loads or moments would be divided by two.

Characteristic load-displacement relationships

Separation of Wall I from Wall II in the y-direction.—The characteristic load-displacement relationship for this separation was ob-

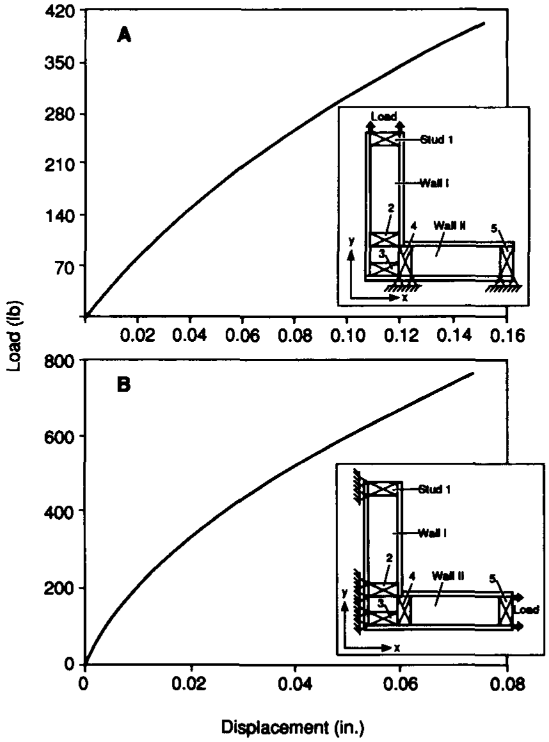

FIG. 8. Characteristic load-displacement relationships for (A) separation of Wall I from Wall II in the y-direction and (B) separation of Wall II from Wall I in the x-direction.

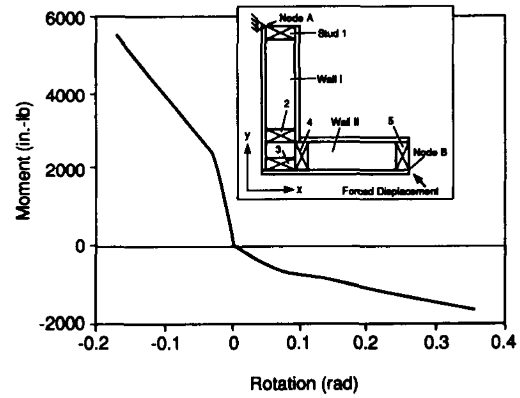

FIG. 9. Characteristic moment-rotation relationship.

tained by moving Wall I and holding Wall II stationary. The boundary conditions and direction of loading are shown in Fig. 8A. Fifteen load steps were applied in 0.01-in. increments, for a total of 0.015 in. The displacement was found by recording the translation of the center of Stud 2 in the y-direction as the load was applied. The results of the loading and boundary conditions are shown in the tracing of Fig. 8A.

Separation of Wall II from Wall I in the x-direction.—The characteristic relationship for this separation was obtained in a similar manner. The loading and boundary conditions are shown in Fig. 8B. The corner nodes of Stud 5 were forced through 15 displacement steps of 0.01 in. each in the x-direction. The slip of the exterior siding was used as the measure of displacement and is shown plotted with load in Fig. 8B.

Characteristic moment-rotation relationship

This relationship was obtained by setting the same boundary conditions as in the original finite-element model. Node A was fixed against translation but was free to rotate as Node B was displaced toward it (Fig. 9). Unlike the original model, the modified model was not loaded to form a hysteresis loop. Instead, it was first loaded to close the corner. As with the earlier model, the closing stiffness was much greater than the opening stiffness. The results are shown in the tracing of Fig. 9.

The rotation for this relationship was obtained by following the paths of the mid-site nodes located on the edges of Studs 2 and 4. For Stud 2, these two nodes were followed in the y-direction and divided by 3.5 in. to give rotation in radians. A similar procedure was followed to obtain rotation of Stud 4. The two rotations were combined to find the rotation of one stud relative to the other.

The centers of rotation for the connection are about two separate points, depending on whether the connection is closing or opening. When the connection is closing, the connection rotates about the point where Studs 2 and 4 contact. However, when the corner is opening, the center of rotation is about the outside corner of Stud 3. Because of this duality, the moments for each load case were found in a different way: The load was always in the same location and acting at Node B on the line between A to B; the moment arm for each case was the distance from the center of rotation to where it intersected the line of force at a right angle. This distance was 11.3 in. when the connection was closing and 12.7 in. when the connection was opening.

CONCLUSIONS

The finite-element model made it possible to obtain characteristic nonlinear load-displacement and moment-rotation relationships to be used as nonlinear springs in a full-structure model of a light-frame wood building. With this method, each 24-in. section of the connection can be replaced by a set of energetically equivalent nonlinear springs comprised of just two nodes. The benefits to the computational efficiency of the full-structure model are obvious when one considers that the original detailed model included 182 nodes at each connection. The other connections in the full-structure model may be obtained by a similar process.

REFERENCES

American Society for Testing and Materials (ASTM). 1989. Standard methods of testing structural panels in flexure. D3043-87. Pages 417–427 *in* Annual book of standards, vol. 04.09. ASTM, Philadelphia, PA.

———. 1990. Standard test methods for physical testing of gypsum board products and gypsum lath. C473-87a. Pages 251–261 *in* Annual book of standards, vol. 04.01. ASTM, Philadelphia, PA.

Bodig, J., and B. A. Jayne. 1982. Mechanics of wood and wood composites. Van Nostrand Reinhold Co., New York, NY. 712 pp.

Delsalvo, G. J., and R. W. Gorman. 1989. ANSYS engineering system user's manual, Version 4.4, vol. I. Swanson Analysis Systems, Houston, PA.

Groom, K. M. 1992. Nonlinear finite-element modeling of intercomponent connections in light-frame wood structures. M.S. thesis, Oregon State University, Corvallis, OR. 167 pp.

Jenkins, J. L., A. Polensek, and K. W. Bastendorff. 1979. Stiffness of nailed wall joints under short and long term lateral loads. Wood Sci. 11(3):145–154.

Kasal, B. 1992. A nonlinear three-dimensional finite-element model of a light-frame wood structure. Ph.D. thesis, Oregon State University, Corvallis, OR. 316 pp.

Phillips, T. J. 1990. Load sharing characteristics of three-dimensional wood diaphragms. M.S. thesis, Washington State University, Pullman, WA. 236 pp.

Polensek, A., and K. M. Bastendorff. 1987. Damping in nailed joints of light-frame wood buildings. Wood Fiber Sci. 19(2):110–125.

———, and B. D. Schimel. 1986. Rotational restraint of wood-stud wall supports. J. Struct. Eng. 112(6):1247–1262.